

Antihydrogen Physics at ALPHA/CERN¹

C.L. Cesar, G.B. Andresen, W. Bertsche, P.D. Bowe, C.C. Bray, E. Butler, S. Chapman, M. Charlton, J. Fajans, M.C. Fujiwara, R. Funakoshi, D.R. Gill, J.S. Hangst, W.N. Hardy, R.S. Hayano, M.E. Hayden, A.J. Humphries, R. Hydromako, M.J. Jenkins, L.V. Jørgensen, L. Kurchaninov, R. Lambo, N. Madsen, P. Nolan, K. Olchanski, A. Olin, R.D. Page, A. Povilus, P. Pusa, F. Robicheaux, E. Sarid, S. Seif El Nasr, D.M. Silveira, J.W. Storey, R.I. Thompson, D.P. van der Werf, J.S. Wurtele, and Y. Yamazaki

Abstract: Cold antihydrogen has been produced at CERN (Amoretti et al. (Nature, **419**, 456 (2002)), Gabrielse et al. (Phys. Rev. Lett. **89**, 213401 (2002))), with the aim of performing a high-precision spectroscopic comparison with hydrogen as a test of the CPT symmetry. Hydrogen, a unique system used for the development of quantum mechanics and quantum electrodynamics, has been continuously used to produce high-precision tests of theories and measurements of fundamental constants and can lead to a very sensitive search for CPT violation. After the initial production of cold antihydrogen atoms by the ATHENA group, the ALPHA Collaboration (<http://alpha.web.cern.ch/>) has set forth on an experiment to trap and perform high-resolution laser spectroscopy on the 1S-2S transition of both atoms. In this contribution, we will review the motivations, goals, techniques, and recent developments towards this fundamental physics test. We present new discussion on predicted lineshapes for the 1S-2S spectroscopy of trapped atoms in a regime not discussed before.

PACS Nos: 36.10.-k, 32.60.+i, 37.10.Gh

Résumé : Nous avons produit de l'anti-hydrogène au CERN (Amoretti et al. (Nature, **419**, 456 (2002)), Gabrielse et al. (Phys. Rev. Lett. **89**, 213401 (2002))), pour faire des comparaisons spectroscopiques de haute précision avec l'hydrogène dans le cadre d'un test de la symétrie CPT. L'hydrogène, qui a joué un rôle unique dans le développement de la mécanique quantique et de l'électrodynamique quantique, a été utilisé continuellement dans des tests de haute précision des théories et des mesures des constantes fondamentales et peut nous conduire à une recherche très précise de la violation CPT. Après que le groupe ATHENA ait produit l'anti-hydrogène froid, l'équipe ALPHA (<http://alpha.web.cern.ch/>) a développé un montage pour piéger les deux types d'atome et faire des mesures de spectroscopie laser de haute précision des transitions 1S-2S dans les deux types d'atomes. Nous passons ici en revue les motivations, les buts, les techniques et les développements récents de ce test fondamental en physique. Nous présentons de nouvelles idées sur la forme des lignes en spectroscopie 1S-2S pour des atomes piégés dans un régime qui n'a pas encore été discuté.

[Traduit par la Rédaction]

Received 4 November 2008. Accepted 25 November 2008. Published on the NRC Research Press Web site at cjp.nrc.ca on 1 October 2009.

C. Cesar² and R. Lambo. Instituto de Física, Universidade Federal do Rio de Janeiro, Rio de Janeiro 21941-972, Brazil.

G. Andresen, P. Bowe, and J. Hangst. Department of Physics and Astronomy, Aarhus University, DK-8000 Aarhus C, Denmark.

W. Bertsche, E. Butler, M. Charlton, A. Humphries, M. Jenkins, L. Jørgensen, N. Madsen, and D. van der Werf. Department of Physics, Swansea University, Swansea SA2 8PP, United Kingdom.

C. Bray, S. Chapman, J. Fajans, A. Povilus, and J. Wurtele. Department of Physics, University of California at Berkeley, Berkeley, CA 94720-7300, USA.

M. Fujiwara, D. Gill, L. Kurchaninov, K. Olchanski, A. Olin, and J. Storey. TRIUMF, 4004 Wesbrook Mall, Vancouver, BC V6T 2A3, Canada.

R. Funakoshi and R. Hayano. Department of Physics, University of Tokyo, Tokyo 113-0033, Japan.

W. Hardy and S.S. ElNasr. Department of Physics and Astronomy, University of British Columbia, Vancouver BC V6T 1Z4, Canada.

M. Hayden. Department of Physics, Simon Fraser University, Burnaby BC V5A 1S6, Canada.

R. Hydromako and R. Thompson. Department of Physics and Astronomy, University of Calgary, Calgary AB T2N 1N4, Canada.

P. Nolan, R.D. Page, and P. Pusa. Department of Physics, University of Liverpool, Liverpool L69 7ZE, UK.

F. Robicheaux. Department of Physics, Auburn University, Auburn, AL 36849-5311, USA.

E. Sarid. Department of Physics, NRCN-Nuclear Research Center Negev, Beer Sheva, IL-84190, Israel.

D. Silveira. Graduate School of Arts and Sciences, University of Tokyo, 3-8-1 Komaba, Meguro, Tokyo, 153-8902, Japan.

Y. Yamazaki. Atomic Physics Laboratory, RIKEN, Saitama 351-0198, Japan.

¹This paper was presented at the International Conference on Precision Physics of Simple Atomic Systems, held at University of Windsor, Windsor, Ontario, Canada on 21–26 July 2008.

²Corresponding author (e-mail: lenz@if.ufrj.br).

1. Introduction

The very fundamental discrete symmetry of CPT, standing for the simultaneous operations of charge conjugation (C), parity inversion (P), and time reversal (T), is a base for quantum field theories and the standard model of physics [1]. Many different tests of CPT violation comparing matter and antimatter have so far yielded a null result. CPT symmetry predicts, among other things, that the atom and its conjugate, the anti-atom, should have absolutely the same properties, including their energy levels and the lifetimes of these levels. A simple atomic system such as hydrogen, with its very high quality-factor transition 1S-2S presently yielding precisions of parts in 10^{14} [2], and with the possibility of making its antimatter conjugate, seems like a perfect candidate to look for CPT violation.

While CPT has survived every experimental check to date, it is clear that we do not yet have a good model for the Universe, its asymmetry in the natural abundance of matter and antimatter and explanations for dark matter and neutrino mass. Clearly, this is a time where technology allows for investigations of higher sensitivity and possibly new and revolutionary discoveries. With very high precision measurements one might be able to uncover even minuscule effects. This is the main motivation of the experiment we describe here.

The ALPHA Collaboration started at the Antiproton Decelerator (AD) at CERN in 2006, with the goal of performing a high-precision spectroscopic comparison between hydrogen and antihydrogen. Half of its team were in the ATHENA Collaboration, also at the AD, where we produced the first cold antihydrogen atoms [3], quickly followed by the ATRAP Collaboration [4]. The anti-atoms were made from cold antiprotons and positrons in a Penning–Malmberg trap for these charged species, whereupon the anti-atoms were free to annihilate at the trap walls. At ALPHA, a surrounding magnetic trap for the neutral anti-atoms should allow for holding the coldest antihydrogen atoms produced.

In this paper we describe recent developments in the ALPHA experiment and relevant issues with regards to the high-precision comparison of hydrogen and antihydrogen.

2. Production of cold antihydrogen in a neutral atom trapping environment

The first cold antihydrogen atoms were produced in the ATHENA experiment in the so-called nested Penning trap, where thousands of antiprotons were shot at a few electronvolts through a dense sample of cryogenically cold positrons. The typical, most favored, process for the formation of a bound atomic state is through the 3-body collision involving an antiproton and two positrons, whereby the antiproton can capture one of the positrons, while the other leaves, carrying excess momentum and energy. The magnetic field required for holding this cold and dense plasma in the Penning trap has to be quite symmetric and homogeneous, and thus, it seems in principle, incompatible with the highly inhomogeneous field required for magnetic trapping of the neutral atoms.

This was the first challenge for the ALPHA Collaboration, whose immediate goal was to produce and trap the cold antihydrogen atoms. After simulations and tests [5],

the decision was made to pursue the construction of magnetic trap using a bias field and mirror coils axially superposed with an octupole, rather than the usual quadrupole of the Ioffe–Pritchard trap. The octupolar field adds very little asymmetry at the center of the Penning trap, and if the cold plasma sample can be kept at very small radius and reasonably short axial lengths there is negligible loss. It was in such an environment that we were able to demonstrate the production of cold antihydrogen recently [6].

The challenge now is to improve the mixing procedure to produce cold enough antihydrogen to be able to trap some of the anti-atoms. The ALPHA apparatus incorporates some interesting features for the detection of the trapped antihydrogen. First, a silicon vertex detector is able to produce images of the annihilated antiprotons with a low background noise, by detecting the multiple charged pions produced simultaneously in the annihilation. A typical mixing scheme produces cold, but not trapped, antihydrogen, which can escape the trap and annihilate at the walls. The three-dimensional image, produced by detector, of the antiproton annihilations can be used to study asymmetries in the velocity distribution of the created antihydrogen atoms as in [7] for instance. Second, our octupole magnet has a low enough inductance that it can be shut down in times as short as 10 ms. This facilitates the search for trapped anti-atoms by monitoring detector signals directly after the trap shutdown, as shown in ref. 8.

Many issues make the trapping of antihydrogen challenging. The magnetic trapping energy interaction is given by the interaction of the atom's magnetic moment μ with the inhomogeneous magnetic field $\mathbf{B}(\mathbf{r})$ as,

$$H_B = -\mu \cdot \mathbf{B}(\mathbf{r}) \quad (1)$$

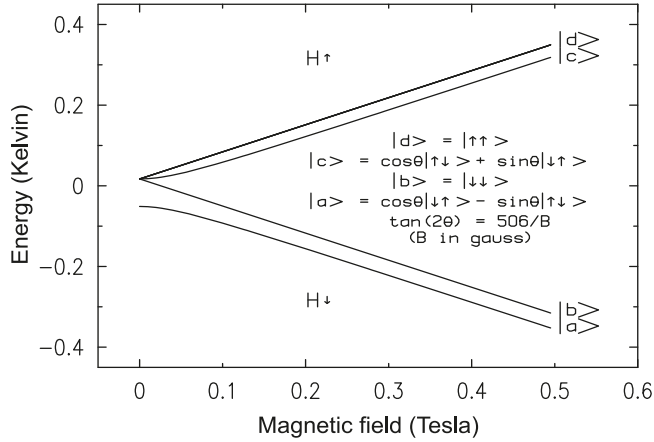
The typical hyperfine diagram of the 1S state of hydrogen, with its four states labeled $\{|a\rangle, |b\rangle, |c\rangle, |d\rangle\}$, is shown in Fig. 1. The trap depth for an atom whose magnetic moment is oriented against the magnetic field is then given by,

$$E_t = \mu [B(\mathbf{r}_w) - B(0)] \quad (2)$$

where $B(\mathbf{r}_w)$ is the minimum field barrier along an escape route — typically made to coincide with the field at the wall — and $B(0)$ is the field minimum in the trap center, where the atoms are created. Only if the initial kinetic energy of the atom is less than this will it find itself trapped. For the $1S_d$ state, this trapping energy is 0.67 K for 1 T of field depth. The need for a high bias field in the Penning trap for the capture and cooling of the positrons, electrons, and antiprotons results in the sacrifice of some depth for the magnetic trap. Pushing the superconducting magnet technology and with some creative construction that separates the antiproton capture and cooling region from the antiproton–positron mixing region — thus allowing a lower bias field in the mixing region — we were able to achieve a magnetic trap depth of typically 0.8 K, for a $1 \mu_B$ (Bohr magneton) atom. This energy is small, putting stringent limits on the experiment, which manipulates plasmas with eV levels of energy.

If the atom is produced in a high magnetic moment state, such as Rydberg circular state, the trapping energy can be much higher than this, provided it is in a low-field seeking

Fig. 1. Hyperfine diagram of the 1S state in hydrogen, with the energy given in Kelvin. The doubly polarized state $|d\rangle$ is the one that typically survives in a high density H trap. The 2S state diagram would be visually undifferentiated, but there is actually a small correction to the magnetic moments that causes a slight residual Zeeman shift and broadening on the 1S $_d$ -2S $_d$ spectrum.



state. However, theoretical simulations predict that only a small fraction of the generated antihydrogen atoms will have the appropriate magnetic moment orientations and states [9].

Small temperature rises due to plasma manipulations, and also the plasma dynamics that occur during mixing, may pose serious impediments to producing anti-atoms in the Kelvin temperature regime. Learning to diagnose, deal, and identify which of these issues are important is a time-consuming process. However, to date we have identified no fundamental physics impediment or “Maxwell demon” that would lose all the created atoms, such that, given time, we still anticipate the trapping of anti-matter atoms.

3. Proposal for first cooling of high angular momentum cold antihydrogen

In the three-body combination process, in which a collision of two positrons and one antiproton results in the formation of an antihydrogen atom, phase-space considerations favor the initial formation of high angular momentum states [9]. If one considers the fraction of the formed atoms that are trapped, which from energy considerations is likely to be comprised of those that have a high magnetic moment, one can follow their dynamics, right after formation, through the trap. These high angular momentum states will most likely decay slowly towards the ground state. In this process, they may lose or gain mean kinetic energy, which we will loosely refer to as a “temperature”. When the atom decays by spontaneous emission, it changes its angular momentum by one unit of \hbar . In this process, it is likely to decrease the magnitude of the projection of its angular momentum along the magnetic field. Suppose the trap is such that the difference in magnetic energy between adjacent magnetic moment states at the trap edges is twice that at the trap center. If the atom decays at the edge of the trap, then it is more likely to lose a high potential energy while going to a slightly shallower trap – resulting in cooling – while if it decays at the trap center, it typically loses little potential energy, while the trap depth has decreased significantly. Spontaneous emission

is most likely to happen near the trap edges, on turning points, where the atoms spend most of their time in the trap. This process has been simulated [10, 11], showing the predicted natural automatic cooling because of spontaneous emission.

If this process of decay could be enhanced at the turning points of the atoms in the trap, improved cooling could result. This has been discussed at length elsewhere, resulting in a proposal to use microwaves resonant near the trap edges to enhance this cooling process [12]. Using a simple model as well as a sophisticated simulation with the full diamagnetic Hamiltonian, this cooling is confirmed. Without optimizing all the parameters, one can gain from the microwaves about 70% in the number of trapped atoms for an initial magnetic moment of about $25 \mu_B$, at a sample temperature of 16 K. Of course, the higher the initial magnetic moment state, the better the microwave cooling works. Even a small improvement in the number and a decrease in the temperature of trapped antihydrogen atoms will be relevant for the physics program of the experiment.

With trapped atoms and in the absence of the plasmas, which can be discarded after the mixing, one will have times that are long enough to perform other cooling schemes, such as Lyman- α laser cooling [13], or two-photon laser cooling [14], or even attempt other schemes. The further cooling of the sample may make it possible to attain high precision in the spectroscopic comparison of the two conjugate species and thus in the corresponding test of CPT symmetry. It may even point the way to future gravitational experiments with these neutral anti-atoms.

4. Spectroscopy of trapped antihydrogen atoms

Once the first few antihydrogen atoms have been trapped, the drive for spectroscopy can begin. Even with trapped atoms, the challenges for spectroscopy are large. Since the ALPHA setup uses an octupolar magnetic trap, the potential has its largest effect on the antihydrogen when it is near the cell walls, which means that the atoms will occupy most of the cell volume. Thus, a simple analysis of the overlap of the trapped atoms with the focused laser beam already shows the difficulties for the laser excitation, as we discuss below. The other challenges are the residual Zeeman broadening of the 1S-2S transition, even in the correspondingly doubly polarized states, and the time-of-flight broadening.

In what follows, we provide simple estimates of parameters that allow the spectroscopy of a few trapped atoms and discuss optimization of the conditions from trap depths around 1 K. As an atom crosses a laser beam it cannot resolve the laser frequency to better than about $1/\tau_{\text{tof}}$, where τ_{tof} is the so called time-of-flight of the atom through the laser beam, or the observation time. This is the description from a Fourier transform perspective. The problem with this comes with the conservation of energy. This can be easily resolved if one solves the interaction problem more completely and includes the momentum of the atom. In the ultra-cold limit, this process gives rise to interesting features and sidebands in a harmonic trap as fully developed in ref. 15, and as observed in ref. 16.

The regime expected for the first spectroscopy of trapped

anti-atoms will most likely be far from the dense and ultra-cold regime where previous analyses [15, 17] apply best. Here, it is worthwhile to consider some simple estimates of transition rates, line widths and possible optimizations, verify some scaling laws using the simple semiclassical picture [18], and extend the analysis for the case of atoms in a shallow trap.

In the Doppler-free configuration, e.g., two counterpropagating and degenerate photons, the excitation rate for an atom interacting with an intensity I of the retro-reflected linearly polarized laser beam is given by [19],

$$\gamma_{\text{exc}} = 85.7(I^2/\Delta\omega) (\text{cm}^4/W^2)\text{s}^{-2} \quad (3)$$

where $\Delta\omega$ is the instrumental line width of the atomic transition and can be due to just the natural line width in the case of an atom at rest, laser jitter, or a time-of-flight line width if the atom is crossing the laser beam. The time-of-flight broadening (1/e half-width, at the two-photon frequency) for a thermal sample in a box is given by [15, 18],

$$\Delta\omega_{\text{tof}} = \frac{\sqrt{2k_B T/M}}{w(z)} \quad (4)$$

where k_B , T , M , and $w(z)$ are the Boltzmann constant, the temperature, the atomic mass, and the laser beam waist at a position z , respectively.

4.1. Optimization of the beam waist for atoms in a box

A Gaussian laser, with total power P , has a beam waist propagation along the z -axis given by $w(z) = w_0[1+(z/z_R)^2]^{1/2}$, where $z_R = \pi w_0^2/\lambda$ is the Rayleigh length, w_0 is the minimum beam waist, and λ is the laser wavelength. Because of the 2-photon character of the 1S-2S transition, the transition rate is proportional to the intensity squared,

$$I^2 = \{2P/[\pi w^2(z)]\}^2 \exp[-4r^2/w^2(z)]$$

and inversely proportional to the line width. Thus, in the time-of-flight broadening dominated regime, the transition rate per atom is proportional to

$$[P^2/w^3(z)] \exp[-4r^2/w^2(z)]$$

For the total transition rate, the larger the area of the beam ($\sim w^2(z)$) and the longer the sample length the more atoms it interacts with. Therefore, in the case of a box with length $2z_0$ and constant atomic density n , the total transition rate will depend on density, power, and minimum beam waist as [19],

$$\Omega_{\text{exc}}^{(\text{box})} \propto nP^2 \int_{-z_0}^{z_0} \frac{dz}{w(z)} \propto nP^2 w_0 \text{ArcSinh}\left(\frac{z_0 \lambda}{\pi w_0^2}\right) \quad (5)$$

For sample lengths of 2–20 cm, the minimum beam waist that optimizes the total transition rate varies from 20–60 μm and is approximately given by $w_0 \approx \sqrt{2z_0 \lambda / \pi e}$.

4.2. Finding the atoms with the laser

A beam waist of 20–60 μm in an octupolar trap with trap radius of $R_t \sim 22$ mm poses a serious challenge for excitation with a sample temperature as high as the trap depth. A simple estimate of the laser–atom overlap (w_0^2/R_t^2) gives val-

ues of $\sim 10^{-6}$. A rough estimate of the time for the atoms to find and cross the laser beam with a beam waist $w_0 = 20$ μm can be made by considering full ergodicity. An antihydrogen atom at 0.6 K will have a speed of about $u \sim 100$ ms^{-1} and will cross a laser if it is within an impact parameter of w_0 . Thus, a simple estimate of the time it takes for the atom to find the laser, considering the trap as a box, is given by the area of the trap (πR_t^2) divided by $u \times 2w_0$, which gives about 0.4 s. This simple estimate is corroborated by a Monte Carlo simulation using typical trapping fields. This value clearly shows that we can ignore coherence between passes as this time is longer than the natural decay time of the 2S state of 122 ms.

The atom crosses the laser beam in about $2w_0/u \sim 0.4$ μs . The time-of-flight broadening for a single radial speed (u) is given by [15, 18] a Gaussian line shape with a standard deviation line width of $\sqrt{2u/w_0} \sim 8 \times 10^6$ s^{-1} , which gives a $\Delta\omega_{\text{HWHM}} \sim 2\sqrt{\ln 2}u/w_0$. The effective intensity experienced by the anti-atom when traversing the beam for a distance $2w_0$, and also averaging over the impact parameter, is obtained by correcting the power by a factor of 0.44. Thus, the equation for the excitation rate (3) multiplied by the crossing time ($2w_0/u$) provides the excitation probability per pass (Pb_{pass}) (in SI units),

$$\text{Pb}_{\text{pass}} \sim 86 \times 10^{-8} \left(\frac{2 \times 0.44P}{\pi w_0^2}\right)^2 \times \frac{w_0}{2\sqrt{\ln 2}u} \times \frac{2w_0}{u} \quad (6)$$

For a power of 10 mW of 243 nm radiation, as used at MIT to observe trapped hydrogen atoms [16], one obtains an excitation probability of about $\text{Pb}_{\text{pass}} \sim 2 \times 10^{-6}$ per pass. To have a 100% excitation probability, the atom has to cross the laser beam some $1/\text{Pb}_{\text{pass}}$ times and that takes a total time $t_{100\%}$,

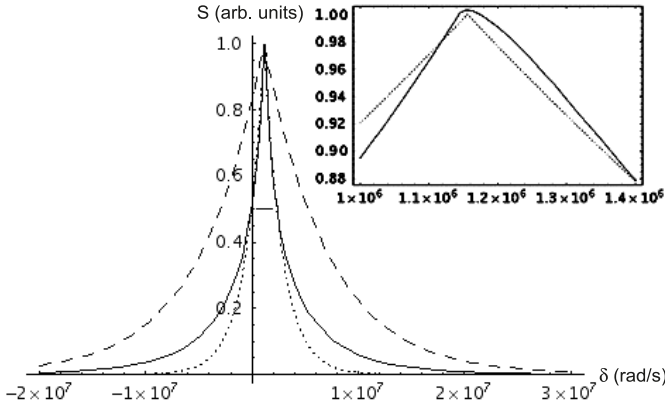
$$t_{100\%} = 190 \times 10^3 \text{ s} \left(\frac{10 \text{ mW}}{P}\right)^2 \left(\frac{R_t}{22 \text{ mm}}\right)^2 \times \left(\frac{u}{100 \text{ ms}^{-1}}\right) \left(\frac{w_0}{20 \mu\text{m}}\right) \quad (7)$$

Clearly, this is an unacceptably long time of many hours (~ 52 , for the parameters above), and experimentally one needs a better set of parameters. The laser power is probably the easiest one to change, to lower $t_{100\%}$. If an enhancement optical cavity is used, the gain will come at the expense of more complexity, and it will be important to fight potential surface contamination effects to avoid spoiling the quality factor of the cavity. A better solution would appear to be to engineer a better, higher power laser. Such a laser system, based on a diode laser followed by a high-power tapered amplifier at 972 nm and frequency quadrupled, is currently under development in Rio. The goal is to achieve one order of magnitude improvement in power at 243 nm over the MIT system mentioned above.

4.3. Time-of-flight broadening for atoms in a shallow trap

In the case of trapped atoms, a more demanding analysis follows because of the non-uniform density of the sample, but especially as a result of the varying magnetic field, which causes an inhomogeneous Zeeman broadening. We

Fig. 2. Spectrum of $1S_d$ - $2S_d$ line in solid line using (12) with the parameters used in the text. The long-dashed line corresponds to a simple time-of-flight broadened line with $w(z) = 20 \mu\text{m}$ and $T = 0.83 \text{ K}$, which is the trap depth used, while the short-dashed uses $T = 0.07 \text{ K}$. Both the dashed lines have been shifted so the peaks coincide with the solid line. The horizontal line segment corresponds to the 224 kHz Zeeman broadening from the full trap depth (see text), which in this case happens to be about half the full width. The detuning (δ) is with respect to the whole $1S$ - $2S$ frequency, that is, at



suppose that the laser is propagating along the axis of the trap. Since the typical laser beam waist is so much smaller than the trap radius, a Zeeman broadening due to the radial extent of the beam is negligible, and we do not need to consider the radial variation of the field or of the density within the laser beam.

4.4. Including the Zeeman shift

In the ultra-cold regime, the Zeeman shift can be easily incorporated in the change of energy of the trapped atomic states [17]. Here, we consider a semiclassical analysis where coherence between passes of the atom through the laser beam can be ignored.

Considering a reasonably dense, thermalized sample, the axial density changes according to a Maxwell–Boltzmann as $n(z) \propto n(0) \exp\{-\mu_B[B(z) - B(0)]\}$, where μ_B is the typical magnetic moment of the $1S_d$ state. The Zeeman shift at a position z is $\delta\omega_Z(z) = 2\pi \times 186 \text{ kHz}[B(z)/1 \text{ Tesla}]$. Here we consider a simplified trap, whose axial confinement is composed of two infinitely thin Helmholtz coils of radius r_0 and at positions $\pm z_0$ giving a field,

$$B(z) = \frac{\mu_0 i}{2} \left(\frac{1}{r_0 \{1 + [(z - z_0)/r_0]^2\}^{3/2}} + \frac{1}{r_0 \{1 + [(z + z_0)/r_0]^2\}^{3/2}} \right) \quad (11)$$

where μ_0 is the vacuum permeability, and i is the effective current through the coil. To mimic the ALPHA trap, we can use $z_0 \approx 120 \text{ mm}$, $r_0 \approx 25 \text{ mm}$, and $i \approx 40 \text{ 000 A}$ for a typical possible condition.

With all these elements, we we can now calculate the full spectrum in the trap by means of the integral below,

$$S_{\text{trap}}(\delta) \propto \int_{-z_M}^{+z_M} dz \frac{\text{Erf}[\sqrt{mv_{\text{max}}^2(z)}/(2k_B T)]}{w(z)} \times \exp\left(\frac{-\mu_B[B(z) - B(0)]}{k_B T}\right) \times \exp\left[\frac{-w(z)|\delta - \delta\omega_Z(z)|}{\sqrt{2k_B T/m} \text{Erf}[\sqrt{mv_{\text{max}}^2(z)}/(2k_B T)]}\right] \quad (12)$$

where δ is the detuning, $(1/2)mv_{\text{max}}^2(z) = \mu_B[B(z_M) - B(z)]$, $z_M \approx z_0$ is the position where the field is maximum, and $\delta\omega_Z(z)$ was defined above.

This $1S_d$ - $2S_d$ line shape can be easily calculated numerically for different conditions. In Fig. 2, we show (solid line) the spectrum of a sample at 2 K in the trap under the conditions discussed above, together with two shifted time-of-flight line shapes for different temperatures, considering just the minimum beam waist $w(z) = w_0$. The long-dashed line corresponds to normal time-of-flight (for a box potential) for a temperature corresponding to the trap depth, or 0.83 K in this case. The short-dashed line uses a temperature of less than 1/10 of that. Both lines have been shifted by $1.156 \times 10^6 \text{ rad/s}$, slightly above the

The result above, for the time-of-flight broadening, is only correct for integration of the radial speed from zero to infinity. In the case of our trapped sample, the integration has to be partial since the Maxwell–Boltzmann distribution is truncated at the trap depth. The time-of-flight broadened excitation rate comes from the following integration [15, 18] over the transverse velocity (v_r) at a given position z (considering the natural line width negligible and with the laser beam waist much smaller than the typical trap dimensions),

$$S_{\text{intg}}^{(\infty)} = \int_0^{\infty} dv_r \exp[-mv_r^2/(2k_B T)] \exp[-\delta^2 w(z)^2/(4v_r^2)] \quad (8)$$

where δ is the detuning. In the case of a trap, the above integral has to be restricted so that the maximum energy allowed is defined by the trap threshold E_t . Taking $B(z)$ as the module of the magnetic field along the z -axis, the integral above is, therefore, restricted to the maximum speed $v_{\text{max}}(z) = \sqrt{2\{E_t - \mu_B[B(z) - B(0)]\}/m}$. The integral above can be easily computed using a program like Mathematica© [20]. The result, in terms of exponentials and complementary error functions, can be fit well by exponentials whose amplitudes and line widths are easily evaluated by expanding the functions around $\delta \sim 0$. The result for a “truncated time-of-flight line width” is,

$$S_{\text{intg}}^{(v_{\text{max}})} \approx \sqrt{\pi k_B T/(2m)} \text{Erf}\left[\sqrt{mv_{\text{max}}^2}/(2k_B T)\right] \times \exp\left(-w_0|\delta|/\left\{\sqrt{2k_B T/m} \text{Erf}\left[\sqrt{mv_{\text{max}}^2}/(2k_B T)\right]\right\}\right) \quad (9)$$

where we can easily identify the 1/e half line width as,

$$\Delta\omega_{\text{tof}}^{\text{trap}} \approx (1/w_0)\sqrt{2k_B T/m} \text{Erf}\left[\sqrt{mv_{\text{max}}^2}/(2k_B T)\right] \quad (10)$$

Zeeman shift due to the bias field at $z = 0$ which is 1.14×10^6 rad/s. The solid line spectrum is slightly asymmetrical around its peak, as shown in the inset, being biased towards higher frequencies as expected from the Zeeman shift. It is interesting to note that the line width is somewhat smaller than expected from a simple time-of-flight at the minimum waist with a temperature corresponding to the trap depth (the long-dashed line). The full, naively expected, Zeeman broadening, given by $\delta\omega(z_0) - \delta\omega(0)$ is shown for comparison. By using larger beam waists, it can be shown that this is also not a limit and narrower lines can be obtained.

For the sake of high-precision spectroscopy then, the biggest systematic effect may arise by determining the shift induced by the bias field or the field at $z = 0$. But this field and the resulting shift can be measured and studied controllably.

In high-precision spectroscopy, given enough signal-to-noise ratio and control over systematic effects, it is common to split a line to parts in 10^3 and even to parts in 10^4 . If the line above could be split to parts in 100, a precision of about 2 kHz (at 121 nm, or 2.5×10^{15} Hz) may be obtained, which could lead to a direct comparison with the corresponding hydrogen frequency of 8 parts in 10^{13} . This is possible with no further cooling of the sample. However, as we have discussed above, the steps to trap sufficient atoms and to be able to interact optically with most of them are themselves challenging.

5. Initial physics with cold trapped antihydrogen

While the goals of the ALPHA experiment are well beyond the precision of parts in 10^{12} mentioned above, even precisions of 100 times less than this will bring improvements in the current status of comparisons between matter and antimatter. Fujiwara et al. [21] have argued that by assuming the expression for the 1S-2S transition, and a perfect charge conjugation symmetry between the atom constituents and their anti-atom counterparts, the comparison between what we call “mass of the electron” and “mass of the positron” would be improved by orders of magnitude from the present 0.8 parts in 10^8 . There is, thus, a new regime of testing nature even for the initial trapped antihydrogen goals.

6. Conclusion

We have described the ALPHA/AD-5 experiment goals and current status. In particular, we have discussed practical issues related to the trapping and spectroscopy of trapped antihydrogen atoms and have outlined some of the major challenges. We have derived expressions to predict the spectra for trapped atoms under conditions more suitable for the initial optical detection of trapped antihydrogen atoms, away from the ultra-cold regime which has already been thoroughly discussed in the past.

References

1. G. Lüders. *Ann. Phys.* **2**, 1 (1957). doi:10.1016/0003-4916(57)90032-5.
2. T. Hänsch. *Rev. Mod. Phys.* **78**, 1297 (2006). doi:10.1103/RevModPhys.78.1297.
3. M. Amoretti, C. Amsler, G. Bonomi, A. Bouchta, P. Bowe, C. Carraro, C.L. Cesar, M. Charlton, M.J.T. Collier, M. Doser, V.

- Filippini, K.S. Fine, A. Fontana, M.C. Fujiwara, R. Funakoshi, P. Genova, J.S. Hangst, R.S. Hayano, M.H. Holzscheiter, L.V. Jørgensen, V. Lagomarsino, R. Landua, D. Lindelöf, E. Lodi Rizzini, M. Macri, N. Madsen, G. Manuzio, M. Marchesotti, P. Montagna, H. Pruys, C. Regenfus, P. Riedler, J. Rochet, A. Rotondi, G. Rouleau, G. Testera, A. Variola, T.L. Watson, and D.P. van der Werf (ATHENA Collaboration). *Nature*, **419**, 456 (2002). doi:10.1038/nature01096. PMID:12368849.
4. G. Gabrielse, N.S. Bowden, P. Oxley, A. Speck, C.H. Storry, J.N. Tan, M. Wessels, D. Grzonka, W. Oelert, G. Schepers, T. Seftick, J. Walz, H. Pittner, T.W. Hänsch, and E.A. Hessels (ATRAP Collaboration). *Phys. Rev. Lett.* **89**, 213401 (2002). doi:10.1103/PhysRevLett.89.213401. PMID:12443407.
5. G.B. Andresen, W. Bertsche, A. Boston, P.D. Bowe, C.L. Cesar, S. Chapman, M. Charlton, M. Chartier, A. Deutsch, J. Fajans, M.C. Fujiwara, R. Funakoshi, D.R. Gill, K. Gomboroff, J.S. Hangst, R.S. Hayano, R. Hydromako, M.J. Jenkins, L.V. Jørgensen, L. Kurchaninov, N. Madsen, P. Nolan, K. Olchanski, A. Olin, A. Povilus, F. Robicheaux, E. Sarid, D.M. Silveira, J.W. Storey, H.H. Telle, R.I. Thompson, D.P. van der Werf, J.S. Wurtele, and Y. Yamazaki (ALPHA Collaboration). *Phys. Rev. Lett.* **98**, 023402 (2007) and refs. cited therein. PMID:17358606. doi:10.1103/PhysRevLett.98.023402.
6. G.B. Andresen, W. Bertsche, A. Boston, P.D. Bowe, C.L. Cesar, S. Chapman, M. Charlton, M. Chartier, A. Deutsch, J. Fajans, M.C. Fujiwara, R. Funakoshi, D.R. Gill, K. Gomboroff, J.S. Hangst, R.S. Hayano, R. Hydromako, M.J. Jenkins, L.V. Jørgensen, L. Kurchaninov, N. Madsen, P. Nolan, K. Olchanski, A. Olin, R.D. Page, A. Povilus, F. Robicheaux, E. Sarid, D.M. Silveira, J.W. Storey, R.I. Thompson, D.P. van der Werf, J.S. Wurtele, and Y. Yamazaki (ALPHA Collaboration). *J. Phys. B At. Mol. Opt. Phys.* **41**, 011001 (2008). doi:10.1088/0953-4075/41/1/011001.
7. N. Madsen, M. Amoretti, C. Amsler, G. Bonomi, P.D. Bowe, C. Carraro, C.L. Cesar, M. Charlton, M. Doser, A. Fontana, M.C. Fujiwara, R. Funakoshi, P. Genova, J.S. Hangst, R.S. Hayano, L.V. Jørgensen, A. Kellerbauer, V. Lagomarsino, R. Landua, E. Lodi-Rizzini, M. Macri, D. Mitchard, P. Montagna, H. Pruys, C. Regenfus, A. Rotondi, G. Testera, A. Variola, L. Venturelli, D.P. van der Werf, Y. Yamazaki, and N. Zurlo (ATHENA Collaboration). *Phys. Rev. Lett.* **94**, 033403 (2005). PMID:15698264. doi:10.1103/PhysRevLett.94.033403.
8. G.B. Andresen, W. Bertsche, P.D. Bowe, C.C. Bray, E. Butler, C.L. Cesar, S. Chapman, M. Charlton, J. Fajans, M.C. Fujiwara, R. Funakoshi, D.R. Gill, J.S. Hangst, W.N. Hardy, R.S. Hayano, M.E. Hayden, A.J. Humphries, R. Hydromako, M.J. Jenkins, L.V. Jørgensen, L. Kurchaninov, R. Lambo, N. Madsen, P. Nolan, K. Olchanski, A. Olin, R.D. Page, A. Povilus, P. Pusa, F. Robicheaux, E. Sarid, S. Seif El Nasr, D.M. Silveira, J.W. Storey, R.I. Thompson, D.P. van der Werf, J.S. Wurtele, and Y. Yamazaki. *AIP Conf. Proc.* **1037**, 241 (2008). doi:10.1063/1.2977843.
9. F. Robicheaux. *Phys. Rev. A*, **70**, 022510 (2004). doi:10.1103/PhysRevA.70.022510.
10. C.L. Taylor, J.J. Zhang, and F. Robicheaux. *J. Phys. B*, **39**, 4945 (2006). doi:10.1088/0953-4075/39/23/012.
11. T. Pohl, H.R. Sadeghpour, Y. Nagata, and Y. Yamazaki. *Phys. Rev. Lett.* **97**, 213001 (2006). doi:10.1103/PhysRevLett.97.213001. PMID:17155740.
12. C.L. Cesar, F. Robicheaux, and N. Zagury. Manuscript in preparation. *Phys. Rev. A*, (2008).
13. I.D. Setija, H.G.C. Werij, O.J. Luiten, M.W. Reynolds, T.W.

- Hijmans, and J.T.M. Walraven. *Phys. Rev. Lett.* **70**, 2257 (1993). doi:10.1103/PhysRevLett.70.2257. PMID:10053515.
14. D. Kielpinski. *Phys. Rev. A*, **73**, 063407 (2006). doi:10.1103/PhysRevA.73.063407.
 15. C.L. Cesar and D. Kleppner. *Phys. Rev. A*, **59**, 4564 (1999). doi:10.1103/PhysRevA.59.4564.
 16. C.L. Cesar, D.G. Fried, T.C. Killian, A.D. Polcyn, J.C. Sandberg, I.A. Yu, T.J. Greytak, D. Kleppner, and J.M. Doyle. *Phys. Rev. Lett.* **77**, 255 (1996). doi:10.1103/PhysRevLett.77.255. PMID:10062405.
 17. C.L. Cesar. *Phys. Rev. A*, **64**, 023418 (2001). doi:10.1103/PhysRevA.64.023418.
 18. F. Biraben, M. Bassini, and B. Cagnac. *J. Phys.* **40**, 445 (1979).
 19. J.C. Sandberg. Ph.D. thesis, Massachusetts Institute of Technology. Unpublished. 1993.
 20. Wolfram Research, Inc. *Mathematica*, Champaign, Ill., USA. 2005.
 21. M.C. Fujiwara, G.B. Andresen, W. Bertsche, P.D. Bowe, C.C. Bray, E. Butler, C.L. Cesar, S. Chapman, M. Charlton, J. Fajans, R. Funakoshi, D.R. Gill, J.S. Hangst, W.N. Hardy, R.S. Hayano, M.E. Hayden, A.J. Humphries, R. Hydomako, M.J. Jenkins, L.V. Jørgensen, L. Kurchaninov, W. Lai, R. Lambo, N. Madsen, P. Nolan, K. Olchanski, A. Olin, A. Povilus, P. Pusa, F. Robicheaux, E. Sarid, S. Seif El Nasr, D.M. Silveira, J.W. Storey, R.I. Thompson, D.P. van der Werf, L. Wasilenko, J.S. Wurtele, and Y. Yamazaki. *AIP Conf. Proc.* **1037**, 208 (2008). doi:10.1063/1.2977840.